UCRL- 88899 REV. 1
PREPRINT

CLASSICAL BINARY-ENCOUNTER COLLISION THEORY FOR ELECTRON-IMPACT IONIZATION OF IONS

Y. T. Lee
Lawrence Livermore National Laboratory
University of California
Livermore, CA 94550

This paper was prepared for submittal to
J.Q.S.R.T.

June, 1985

DISCLAIMER

CLASSICAL BINARY-ENCOUNTER COLLISION THEORY FOR ELECTRON-IMPACT IONIZATION OF IONS

Y. T. Lee
Lawrence Livermore National Laboratory
University of California
Livermore, CA 94550

(Received April 8, 1985)

ABSTRACT

We calculated electron-ion impact ionization using classical binary-encounter collision theory. A differential cross section per unit energy and momentum transfer is derived for two-electron scattering. We obtain the total ionization cross section by integrating this differential cross section over the appropriate energy and momentum transfer and the bound electron-velocity distribution. To simplify the computation, we calculated the bound electron-velocity distribution in the Thomas-Fermi approximation. Comparison with other theoretical calculations shows that our results agree within 50% with the best quantum approximations. Our cross sections and rate coefficients, which are sufficiently accurate for many practical applications, are expressed in computationally simple form.

I. INTRODUCTION

Cross sections for electron-impact ionization of ions are used to determine the non-equilibrium charge-state distribution of hot plasmas such as encountered in fusion and astrophysics research.[1] To model these plasmas, we need ionization cross sections for many highly stripped ions over a wide range of incident electron energies. Since detailed quantum mechanical calculations for many ionization cross sections are not available, the rate coefficients employed in many plasma simulations are derived using semi-empirical formulas. For example, the semi-empirical formula of Sampson and Golden[2] for electron-impact ionization of hydrogenic ions has been applied to compute rate coefficents for partially stripped heavy ions in laser-produced plasmas simulation.[3] The Lotz formula,[4,5] which was obtained by fitting the experimental data available in 1966, is also frequently employed in plasma modeling.

In this paper, we calculate electron-impact ionization of ions in the classical binary-encounter approximation. The basic assumptions are: (1) the incident electron interacts with only one target electron at a time, and (2) the target electron is assumed to be ionized whenever its kinetic energy becomes greater than its binding energy. We derive a classical differential cross section per unit energy and momentum transfer for the scattering of two electrons. The ionization cross section is then obtained by integrating this differential cross section over the appropriate energy and momentum transfer and the bound electron-velocity distribution.

To simplify the computation, we calculate the bound electron distribution in the Thomas-Fermi approximation. Both the kinetic energy and binding energy of a bound electron are given in terms of the Thomas-Fermi potential. This procedure allows us to compute electron-impact ionization cross section for any ion in the periodic table. Using the Thomas-Fermi variable, we also express both the cross section and rate coefficient in a scaled form which is useful for plasma simulation.

To test our method, we have compared our results to a recent Born approximation calculation[6] for partially stripped nickel and gold ions and a distorted-wave Born exchange approximation[7] for Na-like Ar ion. The comparison shows that our results are, in general, within a factor of two of the detailed quantum mechanical calculation. However, our approach is much simpler and also gives results which are sufficiently accurate for many practical applications.

Our calculation does not include any contribution to the ionization cross section due to electron-impact excitation of an inner-subshell electron to a autoionizing state lying above the first ionization threshold. This excitation-autoionization process is currently being investigated theoretically and experimentally in many laboratories. For a few times ionized ion, this indirect ionization process can enhance the cross section by as much as a factor of 20.[8] However, our results should still be applicable for highly stripped heavy ions since for these ions the excitation - autoionization process does not contribute significantly to the ionization cross section.

We have also calculated the energy distribution of secondary electron produced by electron impact ionization using classical binary-encounter collision approximation.

In the next section, we derive a differential cross section per unit energy and momentum transfer for electron binary-encounter collisions. We obtain a general formula for the case where the interaction between the incident electron and the target electrons is not a Coulomb potential. In Sec. III we apply this differential cross section to calculate electron-impact ionization of partially stripped ions. Both the cross section and rate coefficient are written in a scaled form using Thomas-Fermi variables. An expression for the energy distribution of secondary electrons is also given.

II. CLASSICAL BINARY-ENCOUNTER COLLISION THEORY

In this section we derive a differential cross section per unit energy and momentum transfer for the problem of two electrons scattering. This basic cross section is used to calculate electron-ion ionization by considering the collision approximately as a sum of scatterings between two electrons. In our calculation we ignore the interference effect between the electrons.

A. Differential Cross Section

To derive the differential cross section for a momentum transfer $\hbar k$ and simultaneously an energy transfer ΔE from the incident electron to the target electron, we let the incident electron with velocity $\vec{V}_2$ and the target electron initially with velocity $\vec{V}_1$ in the laboratory frame. Their velocities after the collision will be $\vec{V}'_2$ and $\vec{V}'_1$. The center of mass velocity and relative velocity measured in the laboratory frame are

$$\vec{V}_{cm} = \frac{1}{2} (\vec{V}_2 + \vec{V}_1) \quad , \tag{1}$$

$$\vec{V} = \vec{V}_2 - \vec{V}_1 \quad , \tag{2}$$

$$\vec{V}' = \vec{V}_2' - \vec{V}_1' \quad , \tag{3}$$

$$|\vec{V}| = |\vec{V}'| \quad . \tag{4}$$

The momentum transfer in the laboratory frame is given by

$$\hbar^2 k^2 = m^2 |\vec{V}_2' - \vec{V}_2|^2 = \frac{m^2 V^2}{2} (1 - \cos\gamma) \quad , \tag{5}$$

where m = electron mass and γ is the angle between the relative velocities, $\vec{V}$ and $\vec{V}'$ (Fig. 1).

The energy transfer ΔE from the incident electron to the target electron in the laboratory frame is

$$\Delta E = \frac{1}{2} m V_2'^2 - \frac{1}{2} m V_2^2 = \frac{1}{2} m V V_{cm} (\cos\Theta - \cos\Theta') \quad . \tag{6}$$

The angles Θ and Θ' are the azimuth angles of $\vec{V}_1$ and $\vec{V}_2$ in a fixed polar coordinate system where $\vec{V}_{cm}$ is chosen to be the Z-axis. These expressions for momentum and energy transfers are used later to derive the differential cross section for binary-encounter collision.

Let $\sigma(\vec{V}_1,\vec{V}_2)$ be the total cross section describing the scattering of two electrons. Then, the differential cross section $d\sigma(\vec{V}_1, \vec{V}_2)/d(\hbar k)d(\Delta E)$ is related to the total cross section $\sigma(\vec{V}_1,\vec{V}_2)$ by the following relation:

$$\sigma(\vec{V}_1,\vec{V}_2) = \int \frac{d\sigma(\vec{V}_1,\vec{V}_2)}{d(\hbar k)d(\Delta E)} \, d(\hbar k)d(\Delta E) \quad . \tag{7}$$

The integration covers all possible momentum and energy transfer from the incident electron to the target electron in the laboratory frame.

Since the total cross section is a quantity independent of the reference frame, it can also be calculated from the differential cross section in the center of mass frame. The result is

$$\sigma(\vec{V}_1,\vec{V}_2) = \int \left(\frac{d\sigma}{d\Omega}\right)_{cm} \sin\Theta' \, d\Theta' \, d\varphi' \quad , \tag{8}$$

where φ' is the polar angle of the velocity vector $\vec{V}'$ in a fixed coordinate system.

Using Eqs. (5) and (6), we obtain the following differential relations:

$$d\varphi' = \frac{4\hbar^2 k dk}{m^2 V^2 \sin\Theta \, \sin\Theta' \, \sin(\varphi' - \varphi)} \, , \tag{9}$$

$$\sin\Theta' d\Theta' = \frac{2d(\Delta E)}{mV \, V_{cm}} \quad .$$

Substituting these two expressions into Eq. (8) for the total cross section and comparing the result to Eq. (7), we find that

$$\frac{d\sigma(\vec{V}_1,\vec{V}_2)}{d(\hbar k)d(\Delta E)} = \left(\frac{d\sigma}{d\Omega}\right)_{cm} \frac{8\hbar k}{m\, V^3 V_{cm}^3 \sin\Theta \sin\Theta' \sin(\varphi'-\varphi)} \quad . \tag{10}$$

This is a general result for the scattering of two electrons with velocities $\vec{V}_1$, and $\vec{V}_2$. If the electrons interact by a Coulomb potential, the differential cross section in the center of mass frame takes the form

$$(d\sigma/d\Omega)_{cm} = m^2 e^4/(\hbar k)^4 \quad . \tag{11}$$

This cross section is a function of the momentum transfer $\hbar k$ only.

In applying the differential cross section [Eq. (10)] to calculate electron-impact ionization of ions, we assume the target electrons have an isotropic velocity distribution in the laboratory frame. It is useful to define an effective differential cross section of the form

$$V_2 \frac{d\sigma(V_1,V_2)}{d(\hbar k)d(\Delta E)} = \frac{1}{4\pi}\int |\vec{V}_2 - \vec{V}_1| \frac{d\sigma(\vec{V}_1,\vec{V}_2)}{d(\hbar k)d(\Delta E)} \sin\alpha\, d\alpha\, d\Phi \quad , \tag{12}$$

where the angles, α and Φ are the azimuth and polar angles of the vector $\vec{V}_1$ in a fixed coordinate system where $\vec{V}_2$ is chosen to be the Z-axis. The effective differential cross section $d\sigma(V_1,V_2)/d(\hbar k)d(\Delta E)$ depends only on the magnitude of $\vec{V}_1$ and $\vec{V}_2$.

To evaluate the integral, we express the cross section $d\sigma(\vec{V}_1,\vec{V}_2)/d(\hbar k)d(\Delta E)$ as a function of the angle α. From the energy transfer relation shown in Eq. (6), we obtain

$$\sin^2\Theta = \frac{V_2 V_1 \sin^2\alpha}{V\, V_{cm}} \quad , \tag{13}$$

$$\sin^2\Theta' = \frac{4E_2E_1\sin^2\alpha + 4\,(E_2-E_1)\Delta E - 4(\Delta E)^2}{m^2 V^2 V_{cm}^2} \quad . \tag{14}$$

From the momentum transfer relation shown in Eq. (5), we obtain

$$\cos(\varphi-\varphi') = \left(1 - \frac{2(\hbar k)^2}{m^2\, V^2} - \cos\Theta \cos\Theta'\right)/\sin\Theta \sin\Theta' \tag{15}$$

$$\cos\Theta = (V_2^2 - V_1^2)/2VV_{cm} \tag{16}$$

$$\cos\Theta' = (E_2 - E_1 - 2\Delta E)/mV\,V_{cm} \quad . \tag{17}$$

Substituting Eqs. (13) - (17) into the expression for $d\sigma(\vec{V}_1,\vec{V}_2)/d(\hbar k)d(\Delta E)$, we find

$$|\vec{V}_1-\vec{V}_2| \frac{d\sigma(\vec{V}_1,\vec{V}_2)}{d(\hbar k)d(\Delta E)} = \frac{2\sqrt{2m}\,e^4}{\hbar^2k^3(a\cos^2\alpha+b\cos\alpha+c)^{1/2}} \quad , \tag{18}$$

where

$$a = -(\hbar k)^2E_2E_1/2m \quad ,$$

$$b = \sqrt{E_2E_1}/2)\{(\Delta E)^2 - [(\hbar k)^4/4m^2]\} \quad ,$$

$$c = -[(E_2+E_1)/4]\{(\Delta E)^2 + [(\hbar k)^4/4m^2]\} + (\hbar k)^2/4m\,[2E_2E_1 + \Delta E\,(E_2-E_1)] \quad .$$

Using the variable $x = \cos\alpha$, we reduce Eq. (12) for the effective cross section to the form

$$V_2 \frac{d\sigma(V_1,V_2)}{d(\hbar k)d(\Delta E)} = \frac{\sqrt{2m}\,e^4}{\hbar^2k^3}\int_{x_-}^{x_+} \frac{dx}{(ax^2+bx+c)^{1/2}} \quad . \tag{19}$$

The limits of integration are x_+ = AMIN1(1.0, x_1), x_- = AMAX1(-1.0, x_2),

where $x_1 = (-b - \sqrt{b^2-4ac})/2a$, $x_2 = (-b + \sqrt{b^2-4ac})/2a$.

However, it can be shown that $x_1 \leq 1$ and $x_2 \leq -1$ for any allowable energy and momentum transfers.

Then, the integral becomes

$$\int_{x_2}^{x_1} \frac{dx}{(ax^2+bx+c)^{1/2}} = \frac{\pi}{\sqrt{-a}} \sin^{-1}\left(\frac{2ax+b}{\sqrt{b^2-4ac}}\right)\Bigg]_{x_2}^{x_1} = \frac{\pi}{\sqrt{-a}} \quad . \tag{20}$$

Therefore, the effective differential cross section becomes,

$$d\sigma(V_1,V_2)/d(\hbar k)d(\Delta E) = 4\pi m^3 e^4/k_2^2 k_1 \hbar^2 (\hbar k)^4 \quad . \tag{21}$$

Vriens[9] has applied this differential cross section to calculate the energy transfer cross section for electron-atom collision. He claimed it can be derived from the results in Gryzinski's[10] paper. Using the asymptotic solution of the Schördinger equation for the scattering of two electrons, Vriens[11] also obtained a general expression for the differential cross section which includes interference effects. The derivation presented in this paper uses only classical mechanics and is also conceptually very simple. Using our derivation we can easily obtain a simple expression for the effective differential cross section whenever the cross section in the center of mass frame $(d\sigma/d\Omega)_{cm}$ depends only on the magnitude of the momentum transfer. The result is

$$d\sigma/d(\hbar k)d(\Delta E) = [4\pi m/(\hbar k_2)^2 k_1] \left(d\sigma(\hbar k)/d\Omega\right)_{cm} \quad . \tag{22}$$

Generally, if the interaction between electrons is not a coulomb potential, the differential cross section $(d\sigma/d\Omega)_{cm}$ will not be a function of $\hbar k$ only. However, the cross section $(d\sigma/d\Omega)_{cm}$ evaluated in the Born approximation is always a function of $\hbar k$ only. In the next section, we apply Eq. (22) to study the plasma screening effect on electron-ion collisions using the cross section $(d\sigma/d\Omega)_{cm}$ evaluated in the Born approximation.

B. Debye-Hückel Screening

In a plasma the interaction between the incident electron and the target electron is described in terms of the Debye-Hückel potential. If we evaluate the center of mass differential cross section in the Born approximation, then Eq. (22) for the effective differential cross section becomes

$$\frac{d\sigma(V_1,V_2)}{d(\hbar k)d(\Delta E)} = \frac{4\pi m}{(\hbar k_2)^2 k_1} \left(\frac{d\sigma}{d\Omega}\right)_{cm}^{Born}$$

$$= \frac{4\pi m}{(\hbar k_2)^2 k_1} \; \frac{m^2 e^4}{[(\hbar k)^2 + (\hbar k_{DH})^2]^2} \quad , \tag{23}$$

where $k_{DH} = 2\pi/\lambda_{DH}$ (λ_{DH} = the Debye-Hückel screening length).

C. Acceleration of Incident Electron

Both Eqs. (21) and (23) were obtained for scatterings of two free electrons. The effect of the average atomic potential on the incident electron is so far ignored in calculation. We calculate this effect approximately by assuming that the incident electron with initial energy E_2 gains the kinetic energy W before the encounter with the target electron. The kinetic energy gained by the incident electron is exactly equal to $e\varphi(r)$, the average atomic field acting on the electron. In this approximation, the effective differential cross sections Eqs. (21) and (23) become, respectively,

$$\frac{d\sigma(V_1,V_2)}{d(\hbar k)d(\Delta E)} = \frac{2\pi}{(E_2+e\varphi)k_1} \frac{m^2e^4}{(\hbar k)^4} \tag{24}$$

and

$$\frac{d\sigma(V_1,V_2)}{d(\hbar k)d(\Delta E)} = \frac{2\pi}{(E_2+e\varphi)k_1} \frac{m^2e^4}{\left[(\hbar k)^2+(\hbar k_{DH})^2\right]^2} \quad . \tag{25}$$

D. Energy Transfer Cross Section

We obtain the cross section per unit energy transfer by integrating the differential cross section [Eq. (21)] over the momentum transfer allowed by momentum conservation. For a given energy transfer ΔE, we have

$$(\hbar k)_{min} = (2m)^{1/2} [(E_1+\Delta E)^{1/2} - E_1^{1/2}] \quad , \tag{26}$$

$$(\hbar k)_{max} = (2m)^{1/2} [(E_1+ \Delta E)^{1/2} + E_1^{1/2}] \quad , \tag{27}$$

for $E_2 \leq \Delta E + E_1$, and

$$(\hbar k)_{min} = (2m)^{1/2} [(E_2 + \Delta E)^{1/2} - E_2^{1/2}] \quad , \tag{28}$$

$$(\hbar k)_{max} = (2m)^{1/2} [(E_2 + \Delta E)^{1/2} + E_2^{1/2}] \quad , \tag{29}$$

for $E_2 \leq \Delta E + E_1$.

Integrating the differential cross section [Eq. (21)] over the range of momentum transfer given by Eqs. (26)-(29), we find

$$\frac{d\sigma}{d(\Delta E)} = \frac{\pi e^4}{E_2} \left(\frac{1}{(\Delta E)^2} + \frac{4E_1}{3(\Delta E)^3}\right) \tag{30-a}$$

for $E_2 \geq \Delta E + E$ and

$$\frac{d\sigma}{d(\Delta E)} = \frac{\pi e^4}{E_2} \left[\frac{1}{(\Delta E)^2} + \frac{4(E_2-\Delta E)}{3(\Delta E)^2}\right] \left(\frac{E_2-\Delta E}{E_1}\right)^{1/2} \tag{30-b}$$

for $E_2 \leq \Delta E + E_1$.

Equations (28) and (29) have been derived previously by Stabler.[12]

To include the effect of acceleration of the incident electron by the atomic potential, we assume its energy before the encounter collision is $E_2 + e\varphi(r)$. Since the kinetic energy of the target electrons is always less than $e\varphi(r)$, the relation $E_2 + e\varphi \geq \Delta E + E_1$ is always satisfied for $\Delta E \leq E_2$. Then, the cross section per unit energy transfer becomes

$$\frac{d\sigma}{d(\Delta E)} = \frac{\pi e^4}{(E_2+e\varphi)} \left[\frac{1}{(\Delta E)^2} + \frac{4E_1}{3(\Delta E)^3}\right] \tag{31}$$

for $\Delta E \leq E_2$. In the next section we apply this cross section to calculate electron-impact ionization of highly stripped ions. To simplify the calculation we use the atomic potential evaluated in the Thomas-Fermi approximation.

To investigate the plasma screening effect on the cross section per unit energy loss we integrate Eq. (23) over the appropriated momentum transfer. The result can be written as

$$\frac{d\sigma}{d(\Delta E)} = \frac{\pi e^4}{4E_2E_1E_{DH}}\left\{\frac{1 + (1 + \Delta E/E_1)^{1/2}}{(E_{DH}/E_1) + [1 + (1 + \Delta E/E_1)^{1/2}]^2}\right.$$

$$+ \frac{1 - (1 + \Delta E/E_1)^{1/2}}{(E_{DH}/E_1) + [1 - (1+\Delta E/E_1)^{1/2}]^2}$$

$$\left. + \sqrt{\frac{E_1}{E_{DH}}}\tan^{-1}\frac{2(E_1/E_{DH})^{1/2}}{(1+\Delta E/E_{DH})}\right\}, \qquad (32)$$

where $E_{DH} = (\hbar k_{DH})^2/2m$.

In Fig. 2, we plot $d\sigma/d(\Delta E)$ as a function of $\Delta E/E_1$ for k_{DH}/k_1 = 0, 10^{-2}, 10^{-1}, 1.0. Plasma screening decreases the cross section substantially whenever the ratio of the Debye-Hückel screening length λ_{DH} to the orbital radius of the outer bound electron becomes less than ten.

III. ELECTRON COLLISIONAL IONIZATION

In this section we apply the cross section per unit energy transfer to calculate electron-impact ionization of ions. The basic approximations used are: (1) the incident electron interacts with only one target electron at a time, (2) the target electron is assumed to be ionized whenever the energy transfer is greater than its binding energy, (3) the target electron is considered as a free electron during the collision.

In our calculation we assume that the target electrons are independent scattering centers. The assumption is justified if the effective interaction between the incident electron and the target particles occurs in a relatively small region as compared to the atomic dimension. This is certainly the case if the energy transfer to the target electron is large compared to the binding energy.

Using the binary-encounter collision approximation, the ionization cross section is given in terms of the energy transfer cross section as

$$\sigma(E) = \int_0^\infty \int_0^\infty \int_{I(r,\varepsilon)}^{E} \frac{d\sigma(E,\varepsilon)}{d(\Delta E)} \rho(r,\varepsilon)\, d(\Delta E)\, d\varepsilon\, 4\pi r^2 dr \quad , \tag{33}$$

where $\rho(r,\varepsilon)$ is the energy distribution of the target electrons at the radius r and $I(r,\varepsilon)$ is their local ionization potential. The target electrons are assumed to have an isotropic velocity distribution.

To simplify the computation, we calculate the energy distribution of the target electrons using the Thomas-Fermi approximation. This allows us to compute the total ionization cross section without knowing the energy levels of the ion. Using the Thomas-Fermi scaling variables, we also obtain a scaled ionization cross section for any ion in the periodic table.

A. Thomas-Fermi Approximation

In the Thomas-Fermi approximation, the electron energy distribution for an isolated ion is

$$\rho(r,\epsilon)\ d\epsilon = 2d^3p/h^3 = \frac{(2m)^{3/2}}{2\pi\ \hbar^{2/3}}\ \sqrt{\epsilon}\ d\epsilon \tag{34}$$

for $\epsilon \leq \mu + e\varphi(r)$. The quantities μ and $e\varphi(r)$ are the chemical potential and the electrostatic potential of the ion. In our calculation, we also let $e\varphi(r)$ be the atomic potential acting on the incident electron.

The electrostatic potential is obtained from the solution of the following equations:

$$\nabla^2\varphi(r) = 4\pi en(r) \quad , \tag{35}$$

$$n(r) = (1/3\pi^2)\ [2m/\hbar^2]^{3/2}\ (\mu + e\varphi(r))^{3/2} \quad ;$$

the boundary conditions are

$$e\varphi(r) \rightarrow Ze^2/r \text{ as } r \rightarrow 0 \quad ,$$

$$e\varphi(r) = \frac{Z^*e^2}{r} \qquad r > r_0 \quad ,$$

where Z^* is the ionizaton state of the ion. The quantity r_0 is defined to be the radius of the ion at which $n(r_0) = 0$. The chemical potential μ is equal to $-Z^*e^2/r_0$.

In our calculation, we determine the ion radius for a given ionization state using the numerical result in Ref. 13. We then integrate Eq. (35) inward to obtain the electrostatic potential, $e\varphi(r)$.

B. Ionization Cross Section

Using the electron energy distribution function $\rho(r,\varepsilon)$ calculated in the Thomas-Fermi approximation, we obtain the total ionization cross section as

$$\sigma(E) = 4\pi \frac{(2m)^{3/2}}{2\pi\, \hbar^{2/3}} \int_0^{r_o} r^2 dr \int_{\varepsilon_{min}}^{e\varphi+\mu} \sqrt{\varepsilon}\, d\varepsilon \int_{e\varphi-\varepsilon}^{E} \frac{d\sigma(\varepsilon,E)}{d(\Delta E)}\, d(\Delta E) \quad , \tag{36}$$

where ε_{min} = AMAXI(0, $e\varphi$ - E). The term $(e\varphi(r) - \varepsilon)$ is the ionization energy for a group of electrons with kinetic energy ε at the radius r. For the electrons inside the radius r_m which $e\varphi(r_m) = E$, only these electrons with kinetic energy $e\varphi - E \leq \varepsilon \leq \varepsilon\varphi + \mu$ contribute to the ionization.

After algebraic manipulations, we reduce Eq. (36) to a one-dimensional integral of the form:

$$\sigma = 4\pi \frac{(2m)^{3/2}}{2\pi^2 \hbar^3} \frac{\pi e^4}{E} (I_1+I_2) \quad , \tag{37}$$

where

$$I_1 = \int_{r_m}^{\infty} \frac{r^2 dr}{(1 + \frac{e\varphi(r)}{E})} \left[\frac{2}{3} \frac{(e\varphi+\mu)^{3/2}}{-\mu} - \frac{4}{15} \frac{(e\varphi+\mu)^{5/2}}{E^2} - \frac{2}{3} \frac{(e\varphi+\mu)^{3/2}}{E}\right] \quad , \tag{38}$$

$$I_2 = \int_{o}^{r_m} \frac{r^2 dr}{(1 + \frac{e\varphi(r)}{E})} \left[\frac{2}{3} \left(\frac{(e\varphi+\mu)^{3/2}}{-\mu} - \frac{(e\varphi-E)^{3/2}}{E}\right) - \frac{4}{15E^2}\left((\varepsilon\varphi+\mu)^{5/2} - (e\varphi-E)^{5/2}\right) - \frac{2}{3E}\left((e\varphi+\mu)^{3/2} - (e\varphi-E)^{3/2}\right)\right] \quad . \tag{39}$$

We find it convenient to use the following Thomas-Fermi variables:

$$x = Z^{1/3} \, r/b \quad ,$$

$$(Ze^2/x)\,\chi(x) = e\varphi(r) + \mu \quad ,$$

$$b = \left(\frac{3\pi}{4}\right)^{2/3} \frac{a_0}{2} \simeq 0.885_0 a \quad ,$$

where a_0 is the Bohr radius. We can then write the total ionization cross section as,

$$\sigma(E,Z^*,Z) = [4\sqrt{2}\,(b/a_0)^{5/2} a_0{}^2/Z^{1/3}(E/2I_H)]\; F(r_m/r_0,Q) \quad , \qquad (40)$$

where $Q = Z^*/Z$ and I_H = the ionization potential for hydrogen atom.

The universal function $F(r_m/r_0,\,Q)$ is given in terms of the integrals I_1 and I_2, involving the Thomas-Fermi potential and the cross section per unit energy transfer for binary-encounter collision. For a given ionization state, we have evaluated the function F numerically for different values of r_m/r_0. Results are plotted in Fig. 3. This figure summarizes the ionization cross sections for several thousand ions.

C. Ionization Rate Coefficient

The ionization rate coefficient is obtained by integrating the cross section over the electron distribution function. For a Maxwellian electron distribution, the ionization rate coefficient takes the following form:

$$R(Z,Z^*,kT) = \int_{I(Q)}^{\infty} \sigma(E,Z,Z^*)\, \sqrt{\frac{2E}{m}}\, \frac{2}{\sqrt{\pi}}\, \frac{\sqrt{E}}{(kT)^{3/2}}\, e^{-E/kT} dE \quad , \qquad (41)$$

where $I(Q) = Z^* e^2/r_0$ is the ionization potential of the ion.

Substituting Eq. (40) for the cross section into Eq. (41),

$$R = \frac{16\sqrt{2}\,(b/a_o)^{5/2} a_o^{\,2}}{\sqrt{\pi} Z} \left(\frac{2I_H}{m}\right)^{1/2} \left(\frac{I_H b}{e^2}\right) \frac{G(Q,\tilde{kT})}{(\tilde{kT})^{3/2}} , \qquad (42)$$

where $\tilde{kT} = kT/(Z^{4/3}e^2/b)$. The function $G(Q,\tilde{kT})$ is given by

$$G(Q,\tilde{kT}) = \int_0^{y_o} F(y_m/y_o,Q) \exp - \left(\frac{\chi(y_m)}{y_m} + \frac{Q}{y_o} \right)/\tilde{kT}$$

$$\times \left[\frac{\chi(y_m)}{y_m^{\,2}} - \frac{\chi'(y_m)}{y_m} \right] dy_m \quad ,$$

where $y_o = Z^{1/3} r_o/b$ and $y_m = Z^{1/3} r_m/b$.

The ionization rate coefficient given by Eq. (42) scales with the nuclear charge as Z^{-1} if the temperature is scaled as $\tilde{kT}/(Z^{4/3}e^2/b)$. The numerical results for the function $G(Q,\tilde{kT})$ are plotted in Fig. 4.

D. Comparison with Other Calculations

To test our method, we compare our results to other theoretical calculations. In Figs. 5 and 6, we plot our cross sections for nickel and gold ions together with the Born cross sections computed by E. J. McGuire.[6] In his calculation both the ionization energy and wavefunction were obtained from the solution of the Schrödinger equation using Herman-Skillman potential. The comparison shows that our results are within a factor of two of the Born approximation. However, our calculation is much simpler and does not require knowing the sub-shell binding energies of the ion. The results are expressed in terms of a function which scaled with Q ($Q = Z^*/Z$) and can be used to calculate ionization cross sections for any ion.

Also plotted in Figs. 5 and 6 are cross sections computed using semi-empirical formula of Golden and Sampson for hydrogenic ions.[2] The ionization energies used were obtained from the screened hydrogenic model.[14] In this model the energy levels which depend only on the principal quantum number n are computed using screening constants.[14] The comparison shows that the hydrogenic approximation significantly underestimates the cross section at very high energy, E = 10 keV. This is due to the neglect of sub-shell splittings in the hydrogenic model. For heavy ions such as nickel and gold, the sub-shell splitting energies are large.

Fig. 7 shows the ionization cross section of Na-like Ar ion as a function of energy. Also shown are the cross sections calculated in a distorted-wave Born exchange approximation.[7] In these calculations the electron distorted-wave function was generated using a local energy-dependent potential which includes the direct term of the frozen-core Hartree-Fock and a semi-classical exchange term. Cross sections for 3s ionization only are represented by the dashed curve. Above the inner-shell ionization threshold, the figure shows that inner shell ionization can be a factor of four larger than the 3s ionization. The comparison also shows that our results, which include inner shell ionization, agree within 50% with the distorted-wave calculation.

In Fig. 8 we compare our rate coefficients for ionization of Na-like Ar to a distorted-wave Born exchange calculation. The comparison shows that our results agree reasonably well with the distorted-wave approximation.

E. Secondary Electron Energy Distribution

In many applications of the Boltzmann equation to simulate non-Maxwellian electron distribution in plasmas, one needs to know the energy distribution of the secondary electrons produced by electron-impact ionization of ions. The Boltzmann collisional integral describing the ionization process is usually expressed in terms of the differential ionization cross section $d\sigma/d\varepsilon_s$, where ε_s is the kinetic energy of the secondary electron.

Using the cross section per unit energy transfer derived in Sec. IID, we obtain

$$\frac{d\sigma(E)}{d\varepsilon_s} = 4\pi \frac{(2m)^{3/2}}{2\pi^2\hbar^3} \int_0^\infty \int_{\varepsilon_{min}}^{e\varphi(r)+\mu} \frac{d\sigma(E,\varepsilon)}{d(\Delta E)} \rho(r_1\varepsilon)\sqrt{\varepsilon}d\varepsilon\ r^2dr \quad , \quad (44)$$

where

$$\frac{d\sigma(E,\varepsilon)}{d(\Delta E)} = \frac{\pi e^4}{(E+e\varphi)} \left[\frac{1}{(e\varphi-\varepsilon_s+\varepsilon)^2} + \frac{4}{3}\frac{\varepsilon}{(e\varphi-\varepsilon_s+\varepsilon\ )^3}\right]$$

and ε_{min} = AMAX(0, ε +$e\varphi$ - E). The energy range for the secondary electron is $0 \leq \varepsilon_s \leq E + \mu$.

Integrating over the variables r and ε, we find

$$\left(\frac{Z^{4/3}e^2}{b}\right) \frac{d\sigma(E)}{d\varepsilon_s} = \frac{4\sqrt{2}\ (b/a_0)^{5/2}\ a_0^{\ 2}}{Z^{1/3}\ (E/2I_H)} \quad F_s\left(r_m/r_0,\ Q,\ \ \varepsilon_s/\left(\frac{Z^{4/3}e^2}{b}\right)\right) \quad , \ (45)$$

where F_s is a universal function given in terms of an integral involving the cross section per unit energy transfer and the Thomas-Fermi potential.

We have applied Eq. (45) to calculate the secondary electron energy distribution produced in electron-impact ionization of gold ions. Our results are shown in Fig. 9. For an incident electron with kinetic energy E = 1 kev, an appreciable fraction of secondary electrons are produced with energy greater than the ionization potential.

IV. SUMMARY

We have derived a differential cross section per unit energy and momentum transfer for binary-encounter collisions. We applied this cross section to calculate electron-ion impact ionization by assuming: (1) the incident electron interacts with only one target electron at a time, and (2) the target electron is ionized whenever the energy transfer is greater than its binding energy. In our calculation, the bound electron energy distribution is calculated from a Thomas-Fermi potential. Using the Thomas-Fermi variable, we expressed both the ionization cross section and rate coefficient in a scaled form, which can be used for any ion.

We have compared our results to recent Born and distorted-wave Born exchange calculations for electron-impact ionization of partially stripped ions. The comparison shows that our results agree within a factor of two with the best quantum calculation available. However, our calculation is much simpler than the quantum approximations but yet gives cross sections sufficiently accurate for many applications.

ACKNOWLEDGEMENTS

This work was performed under the auspices of the U.S. Department of Energy by the Lawrence Livermore National Laboratory under contract number W-7405-ENG-48.

REFERENCES

1. C. DeMichelis and M. Mattioli, Nuclear Fusion 21, 677, 1981.
2. D. H. Sampson and L. B. Golden, Ap. J. 161, 321, 1970.
   D. H. Sampson and L. B. Golden, Ap. J. 170, 169, 1971.
   L. B. Golden and D. H. Sampson, Ap. J. 163, 405, 1971.
3. G. B. Zimmerman, in "Laser Program Annual Report," UCRL-50021-77, Vol. 2, Lawrence Livermore National Laboratory, Livermore, CA 1977.
4. W. Lotz, Z. Phys. 216, 241, 1968.
5. W. Lotz, Z. Phys. 220, 466, 1969.
6. E. J. McGuire, Phys. Rev. A20, 455, 1979.
7. S. M. Younger, Phys. Rev. A24, 1272, 1981.
8. R. A. Falk, G. H. Dunn, D. G. Griffin, C. Bottcher, D. C. Gregor, D. H. Crandall, and M. S. Pindzola, Phys. Rev. Lett. 47, 494, 1981.
9. L. Vriens, Phys. Rev. 141, 88, 1966.
10. M. Gryzinski, Phys. Rev. 115, 374, 1959.
11. L. Vriens, Case Studies in Atomic Physics, ed. E. W. McDaniel, 1, 337, 1972.
12. R. C. Stabler, Phys. Rev. 133, A1268, 1964.
13. J. C. Stewart and M. Rotenberg, Phys. Rev. 140, A1508, 1965.
14. W. A. Lokke and W. H. Grasberger, unpublished preprint UCRL-52276, Lawrence Livermore National Laboratory, Livermore, CA 1977.

FIGURE CAPTIONS

Fig. 1. $\vec{V}$ and $\vec{V}'$ are the relative velocities before and after the collision. $\vec{V}_{cm}$ is the center of mass velocity. $\vec{V}_1$ is the initial velocity of the target electron.

Fig. 2. The differential cross section per unit energy transfer is plotted vs. $\Delta E/E$; ΔE = energy transfer and E_1 = kinetic energy of the target electron; $k_{DH} = 2\pi/\lambda_{DH}$, λ_{DH} = Debye-Hückel screening length.

Fig. 3. The universal function $F(r_m/r_0,Q)$ used to calculate ionization cross section [Eq. (40)] is shown.

Fig. 4. The universal function $G(Q,k\tilde{T})$ used to calculate ionization rate coefficient [Eq. (42)] is illustrated.

Fig. 5. The ionization cross section for Ni^{12+} is potted as a function of incident electron energy. The dashed curve represents the scaled Born cross section calculated by E. J. McGuire.[6] The dotten curve was calculated by using the hydrogenic formula of Sampson and Golden.[2] The sub-shell splittings of the energy levels were not included.

Fig. 6. The ionization cross section for Au^{14+} is plotted as a function of incident electron energy. The dashed curve represents the scaled Born cross section calculated by E. J. McGuire.[6] The dotted curve was calculated by using the hydrogenic formula of Sampson and Golden. The sub-shell splittings of the energy levels were not included.

Fig. 7. The ionization cross section for Ar^{7+} is plotted as a function of incident electron energy. The dashed curves represent cross sections calculated by using the distorted-wave Born exchange approximation.[7]

Fig. 8. The ionization rate coefficient for Ar^{7+} is plotted as a function of electron temperature. The dashed curves represents the rate coefficients calculated by using the distorted-wave exchange approximation.[7]

Fig. 9. The secondary electron energy distributions are shown for incident electron energies 1 keV and 4 keV.

0164d/0014E

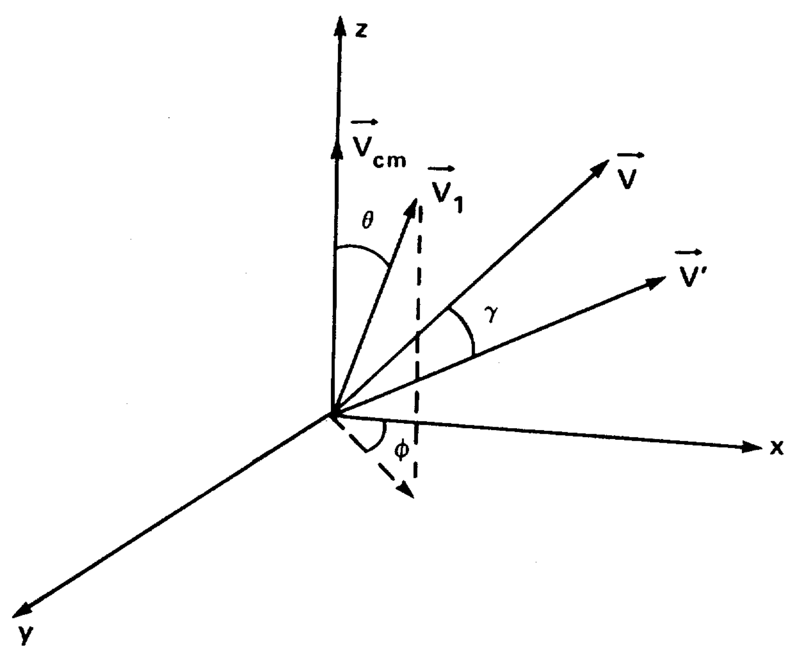

Figure 1

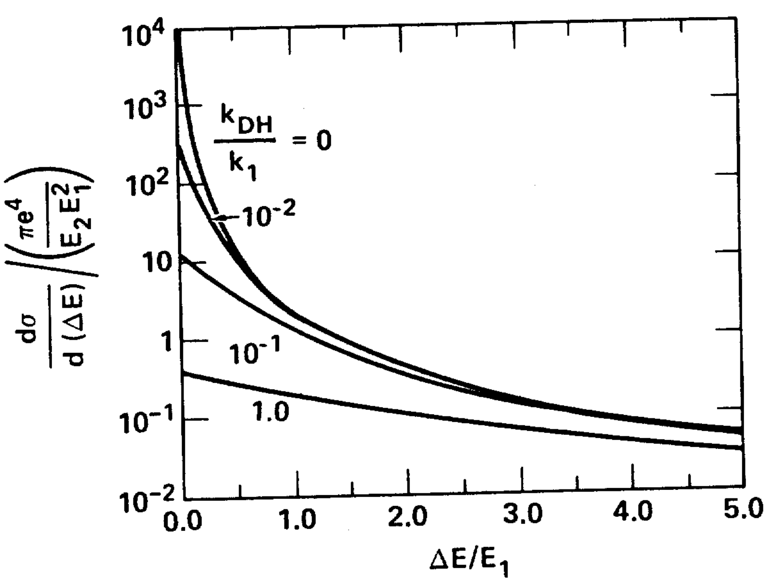

10^4
10^3
10^2
10
1
10^{-1}
10^{-2}
$\frac{k_{DH}}{k_1} = 0$
10^{-2}
10^{-1}
1.0
$\frac{d\sigma}{d(\Delta E)} \Big/ \left(\frac{\pi e^4}{E_2 E_1^2}\right)$
0.0
1.0
2.0
3.0
4.0
5.0
$\Delta E/E_1$

Figure 2

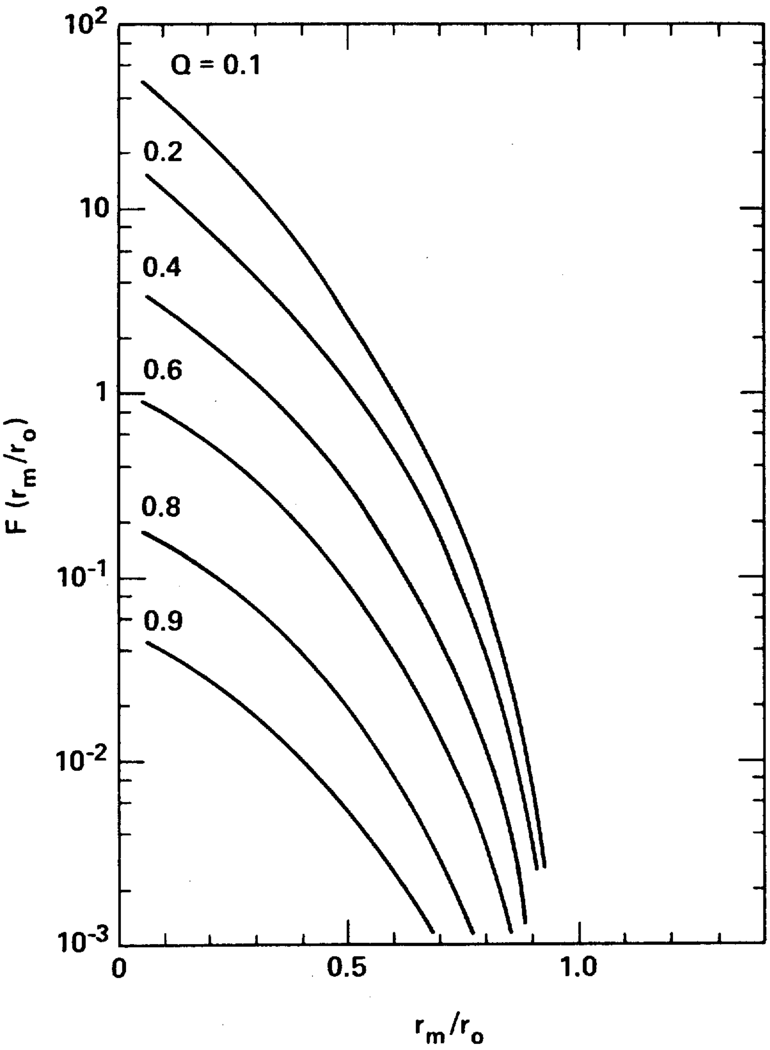

Figure 3

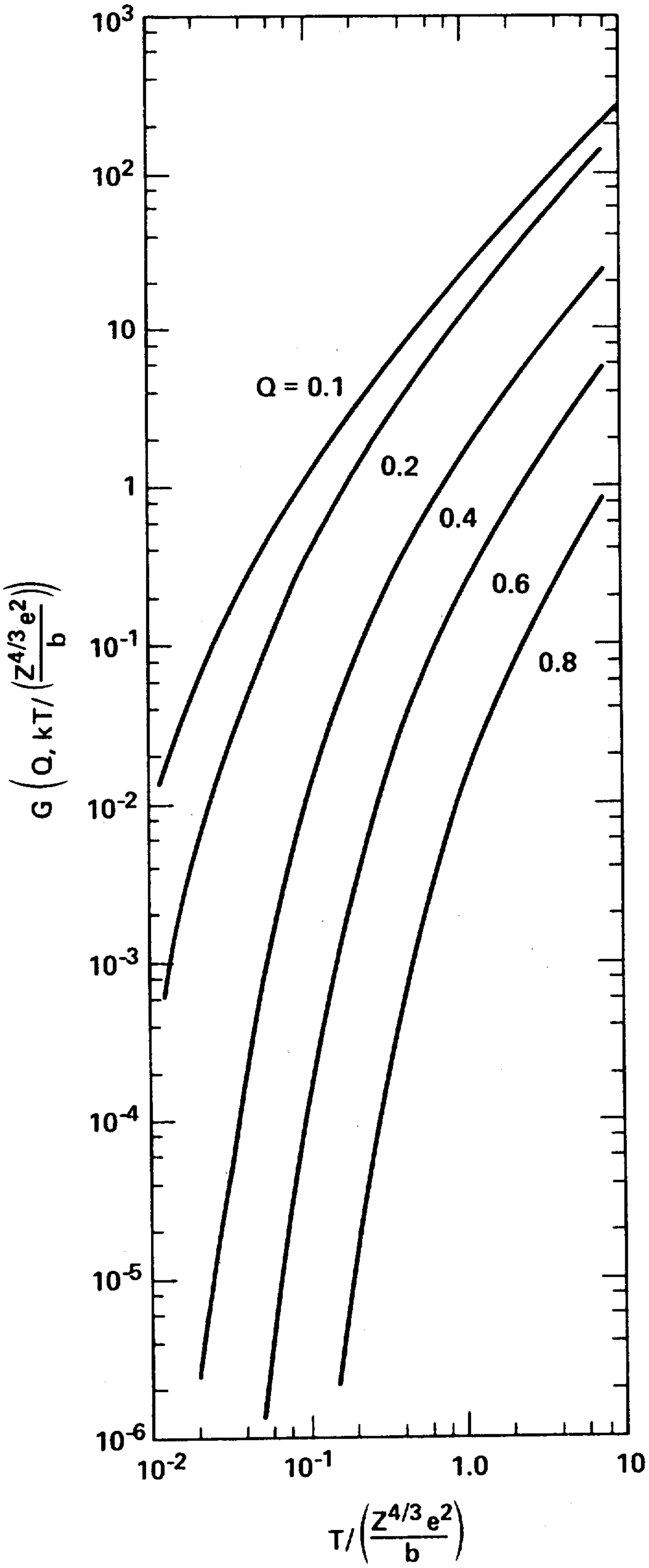

10^3
10^2
10
1
10^-1
10^-2
10^-3
10^-4
10^-5
10^-6
10^-2
10^-1
1.0
10
Q = 0.1
0.2
0.4
0.6
0.8
$G\left(Q, kT/\left(\frac{Z^{4/3}e^2}{b}\right)\right)$
$T/\left(\frac{Z^{4/3}e^2}{b}\right)$

Figure 4

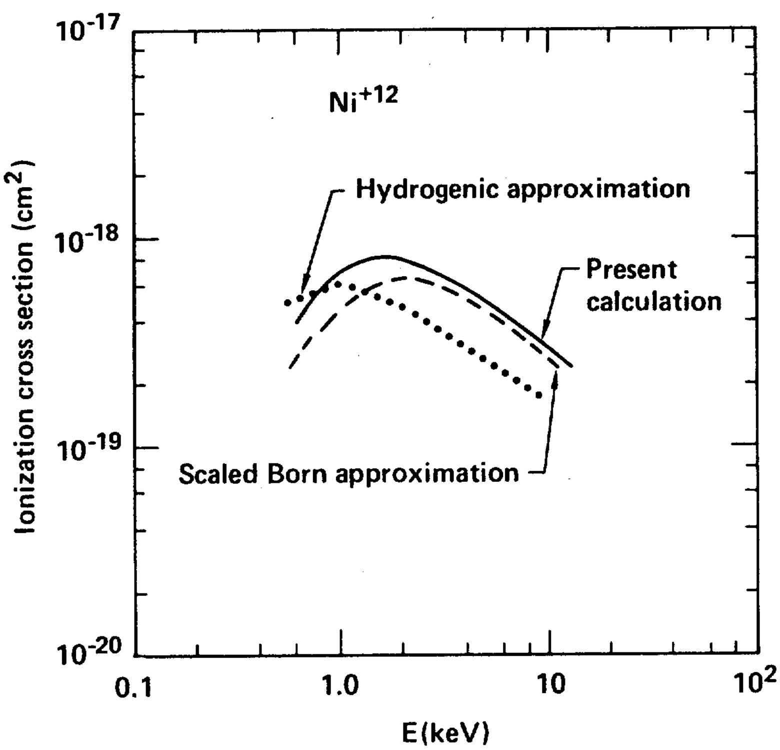

Ni^{+12}
Hydrogenic approximation
Present calculation
Scaled Born approximation
Ionization cross section (cm^2)
10^{-17}
10^{-18}
10^{-19}
10^{-20}
0.1
1.0
10
10^2
E(keV)

Figure 5

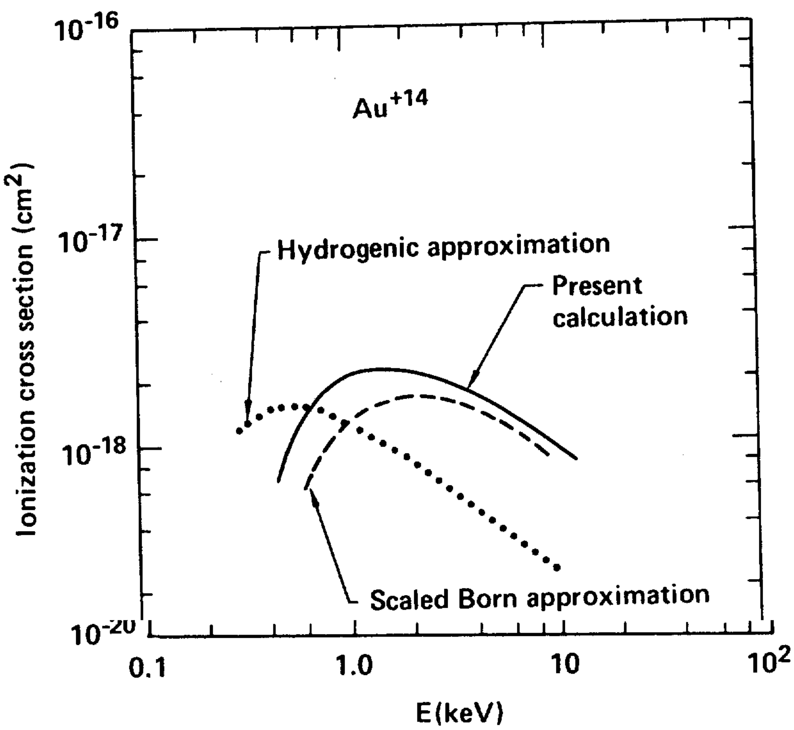
Au+14
Hydrogenic approximation
Present calculation
Scaled Born approximation
Ionization cross section (cm2)
E(keV)
10-16
10-17
10-18
10-20
0.1
1.0
10
102

Figure 5

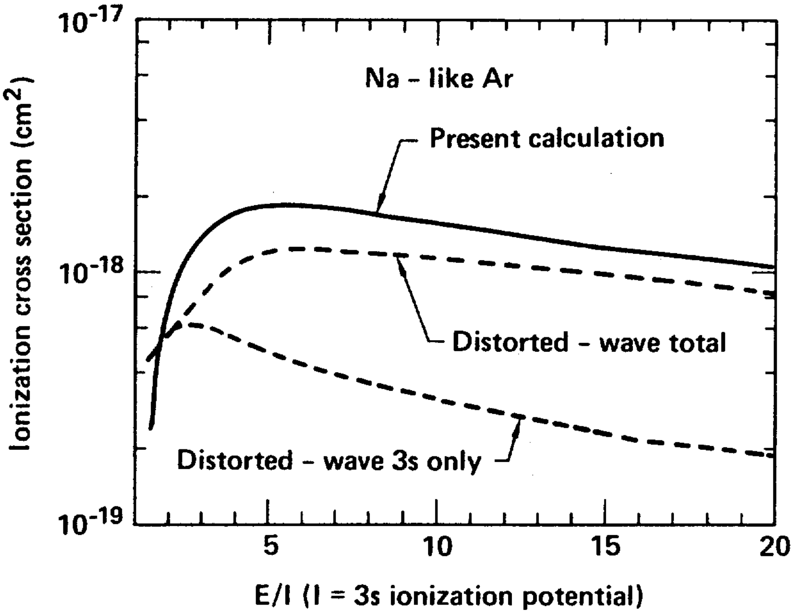

10^{-17}
10^{-18}
10^{-19}
Ionization cross section (cm^2)
Na - like Ar
Present calculation
Distorted - wave total
Distorted - wave 3s only
5
10
15
20
E/I (I = 3s ionization potential)

Figure 7

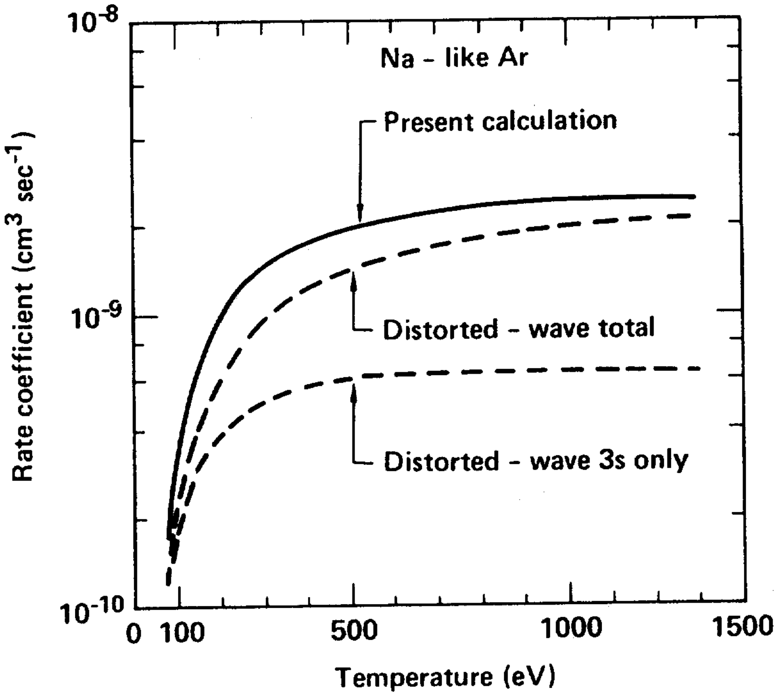

Na - like Ar
Present calculation
Distorted - wave total
Distorted - wave 3s only
10^{-8}
10^{-9}
10^{-10}
Rate coefficient (cm^3 sec^{-1})
0
100
500
1000
1500
Temperature (eV)

Figure 8

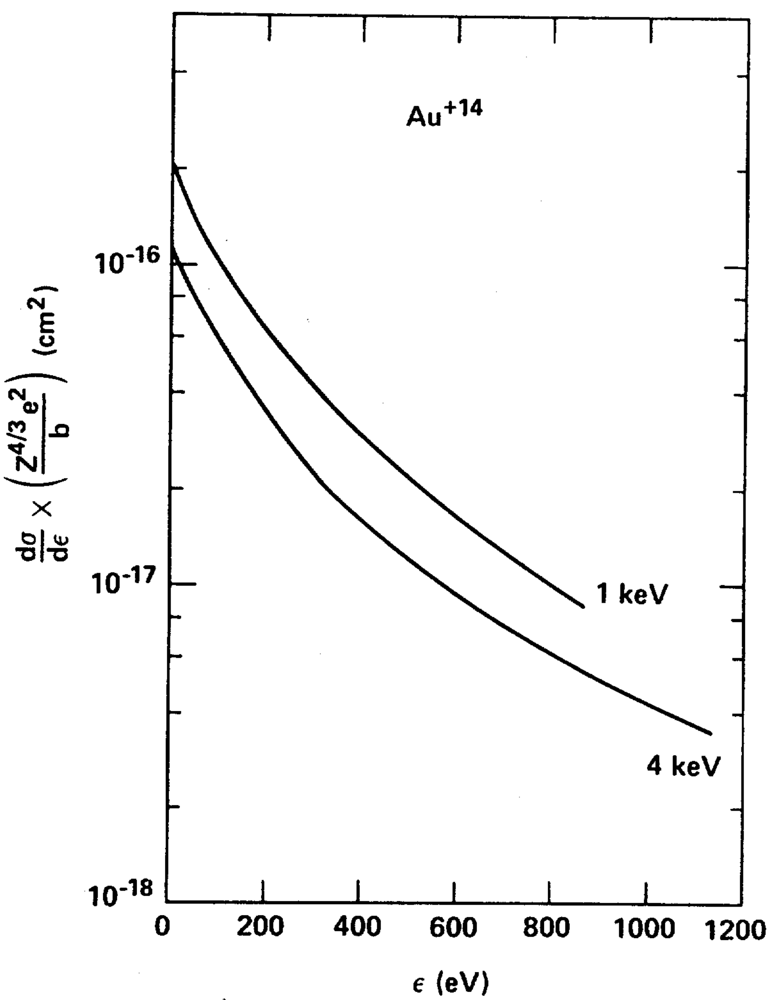

Au^{+14}
10^{-16}
10^{-17}
10^{-18}
$\frac{d\sigma}{d\epsilon} \times \left(\frac{Z^{4/3}e^2}{b}\right)$ (cm^2)
1 keV
4 keV
0
200
400
600
800
1000
1200
ϵ (eV)

Figure 9